Journal of Marine Science and Technology

Volume 25 | Issue 2 Article 9

WELL CONTROL CAPACITY-BASED RISK ANALYSIS OF GAS CUT IN DEEPWATER DRILLING

Yuqiang Xu
College of Petroleum Engineering, China University of Petroleum (Beijing), Beijing, China. College of Petroleum Engineering, China University of Petroleum (East China), Qingdao, Shandong, China.

Zhichuan Guan
College of Petroleum Engineering, China University of Petroleum (East China), Qingdao, Shandong, China., auyuqiang@163.com

Yan Jin
College of Petroleum Engineering, China University of Petroleum (Beijing), Beijing, China.

Hua Pang
College of Petroleum Engineering, China University of Petroleum (East China), Qingdao, Shandong, China.

Yongwang Liu
College of Petroleum Engineering, China University of Petroleum (East China), Qingdao, Shandong, China.

See next page for additional authors

Recommended Citation
Xu, Yuqiang; Guan, Zhichuan; Jin, Yan; Pang, Hua; Liu, Yongwang; Zhang, Bo; and Sheng, Yanan (2017) "WELL CONTROL CAPACITY-BASED RISK ANALYSIS OF GAS CUT IN DEEPWATER DRILLING," *Journal of Marine Science and Technology*: Vol. 25 : Iss. 2 , Article 9.
DOI: 10.6119/JMST-016-1129-2
Available at: https://jmstt.ntou.edu.tw/journal/vol25/iss2/9

WELL CONTROL CAPACITY-BASED RISK ANALYSIS OF GAS CUT IN DEEPWATER DRILLING

Acknowledgements

College of Petroleum Engineering, China University of Petroleum (East China), Qingdao, Shandong, China.

Authors

Yuqiang Xu, Zhichuan Guan, Yan Jin, Hua Pang, Yongwang Liu, Bo Zhang, and Yanan Sheng

Journal of Marine Science and Technology, Vol. 25, No. 2, pp. 205-212 (2017)
DOI: 10.6119/JMST-016-1129-2

WELL CONTROL CAPACITY-BASED RISK ANALYSIS OF GAS CUT IN DEEPWATER DRILLING

Yuqiang Xu[1, 2], Zhichuan Guan[2], Yan Jin[1], Hua Pang[2], Yongwang Liu[2], Bo Zhang[2], and Yanan Sheng[2]

Key words: risk analysis, gas cut, well control capacity, deepwater drilling.

ABSTRACT

Gas cutting typically occurs in deepwater drilling of high-pressure gas reservoirs. If gas cutting is not detected in a timely manner or if the designed well control capacity is insufficient, blowout and other accidents may occur. To address this problem, this paper presents a gas-liquid flow model and kill model in deepwater drilling for the simulation analysis of the gas cutting and killing processes in deepwater drilling. By calculating the maximum allowable killing casing pressure, well control risks under various overflow rates, formation pressures, and kill rates were analyzed, and a well control capacity-based risk analysis method for gas cutting in deepwater drilling was established. In this method, the well control capacity under various drilling conditions was considered. Moreover, by using this method, the well control risk after a gas cut under various conditions can be analyzed to obtain the safe construction parameter range and overflow monitoring index. An example is presented to demonstrate that the established method can be used to recommend safe overflow range, maximum allowable formation pressure prediction error in the current condition, and safety kill rate range under specific working conditions. Thus, the proposed method has practical application in dynamic risk assessment of gas cutting in deepwater drilling.

I. INTRODUCTION

Deepwater oil and gas resources have been majorly explored for fossil energy in the 21st century (Khain and Polyakova, 2004; Xu et al., 2014). Compared with conventional drilling, deepwater drilling entails a more demanding environment with stricter requirements of well control (Botrel and Isambourg, 2001; Chu, 2012). First, as the water depth increases, the formation fracture pressure decreases, safe density window narrows, and kick tolerance decreases (Avelar et al., 2009; Zhou et al., 2012), which is more likely to lead to a gas cut. Second, the deepwater high-static-pressure environment reduces the overall scale of bubbles when they reach the seafloor wellhead, which is not conducive to the early detection of a gas cut by monitoring overflow (Ren et al., 2011). Moreover, the bubbles tend to rapidly rise and expand once they enter the riser. This imposes a large burden on the well control equipment if a killing well is used and may lead to well killing failure because of excessive pressure (Ren et al., 2012).

Recently, researchers have extensively researched on the early detection of gas cuts in deepwater drilling (Zhuo et al., 2009; Chen et al., 2014) and have made great progress in related monitoring equipment and methods. These efforts have aimed to achieve timely warning of a gas cut to implement necessary well control measures and have improved the accuracy and timeliness of gas cut monitoring in deepwater drilling (David et al., 2001; Gupta et al., 2013; Zhou et al., 2013), resulting in more time for subsequent well control (Johnson et al., 2014; Meng et al., 2015). However, many problems, such as safety concerns when the overflow increases and whether the current well control ability meets the safety requirements when a gas cut occurs in deepwater drilling, remain to be investigated. Therefore, in addition to the timely monitoring of gas cuts, analyzing the well control risks under various conditions after a gas cut is necessary to ensure that the gas cut is controlled under the existing conditions. This can provide technical support for overflow monitoring and well control measures under various conditions and can facilitate the dynamic risk assessment of gas cuts in deepwater drilling on the basis of well control capacity.

II. MATERIALS AND METHODS

To study the risks of a gas cut in deepwater drilling, the gas cutting and well killing processes and the influence of various

Paper submitted 10/19/15; revised 11/02/16; accepted 11/29/16. Author for correspondence: Zhichuan Guan (e-mail: auyuqiang@163.com).
[1] College of Petroleum Engineering, China University of Petroleum (Beijing), Beijing, China.
[2] College of Petroleum Engineering, China University of Petroleum (East China), Qingdao, Shandong, China.

factors such as overflow, formation pressure, and killing measurements on well control risks under the existing conditions of well control capacity must be analyzed. Accordingly, a gas-liquid flow model and kill model in deepwater drilling must be established, and the critical indicator–maximum allowable killing casing pressure–must be calculated to analyze the effect of various factors on well control capacity.

1. Gas-Liquid Flow Model and Kill Model in Deepwater Drilling

1) Gas-Liquid Flow Model in Deepwater Drilling

Recently, the wellbore annulus multiphase flow model has been developed to meet the accuracy requirements of design and on-site construction (Gao et al., 2008; Ning et al., 2008; Song and Guan, 2011; Xu et al., 2014). However, because of the unique environmental factors, such as deep water depth and low temperature, associated with deepwater drilling, the temperature accuracy strongly influences the rheology, density, and type of two-phase flow of the annulus drilling fluid (Gao et al., 2008; Ning et al., 2008; Song and Guan, 2011). Therefore, the accuracies of the seawater temperature and wellbore heat transfer models must be improved.

The deepwater temperature model is based on a large set of measured data and has regional characteristics. In this paper, we use the temperature-depth model of South China Sea, established by Gao et al. (2008), as the seawater temperature model.

When the water depth is > 200 m, the temperature at regions with a depth of > 200 m can be calculated using the following formula:

$$T_{\text{sea}} = a_2 + \frac{a_1 - a_2}{1 + e^{(h+a_0)/a_3}} (^{\circ}\text{C}),\ h \geq 200 \text{ m} \tag{1}$$

where a_0, a_1, a_2, and a_3 are dimensionless empirical coefficients: $a_0 = 130.1$, $a_1 = 39.4$, $a_2 = 2.307$, and $a_3 = 402.7$. T_{sea} (°C) is the seawater temperature and h (m) is the seawater depth.

The temperature at regions with a depth of < 200 m can be calculated using various fitted equations according to the season:

$$\text{Spring: } T_{\text{sea}} = \frac{T_S(200-h)+13.7h}{200},\ 0 \leq h < 200 \text{ m} \tag{2}$$

$$\text{Summer: } \begin{cases} T_{\text{sea}} = T_S,\ 0 \leq h < 20 \text{ m}; \\ T_{\text{sea}} = \dfrac{T_S(200-h)+13.7(h-20)}{180},\ 20 \leq h < 200 \text{ m} \end{cases} \tag{3}$$

$$\text{Autumn: } \begin{cases} T_{\text{sea}} = T_S,\ 0 \leq h < 50 \text{ m}; \\ T_{\text{sea}} = \dfrac{T_S(200-h)+13.7(h-50)}{150},\ 50 \leq h < 200 \text{ m} \end{cases} \tag{4}$$

$$\text{Winter: } \begin{cases} T_{\text{sea}} = T_S,\ 0 \leq h < 100 \text{ m}; \\ T_{\text{sea}} = \dfrac{T_S(200-h)+13.7(h-100)}{100},\ 100 \leq h < 200 \text{ m} \end{cases} \tag{5}$$

where T_S (°C) is the sea surface temperature . Because Eqs. (2)-(5) are empirical fitted equations, the units of T_s and h should not be considered in the calculation process.

Unsteady wellbore multiphase flow control equations in deepwater drilling were established on the basis of the drift flow model described by Sun et al. (2013). The specific model has been discussed in the relevant literature (Song and Guan, 2011; Sun et al., 2013) and is therefore not detailed in this paper.

2) Well Killing Model in Deepwater Drilling

The most commonly used well killing methods include the engineer's method, driller's method, and circulate and weight method, and each method has its unique characteristics (Kerr, 2010; Luo et al., 2011). The driller's method, which mainly comprises the following seven stages, is used in this study:

(1) The original drilling fluid replaces seawater within a choke;
(2) The top of the gas column appears at the seafloor BOP (blowout preventer);
(3) The top of the gas column reaches the choker line top;
(4) The bottom of the gas column appears at the seafloor BOP;
(5) The bottom of the gas column reaches the choker line top;
(6) The killing fluid is injected from the wellhead and reaches the bit; and
(7) The killing fluid reaches the choker line top.

Stages (1)-(5) constitute the first loop cycle, and Stages (6)-(7) constitute the second loop cycle. At the end of the second loop cycle, if the casing pressure drops to 0, it indicates that well killing has been achieved; otherwise, well killing should be continued until the casing pressure drops to 0.

Accordingly, the well kill model combined with the two-phase flow model was established when gas cutting occurred in deepwater drilling. The following are the continuity equations in various phases:

Gas continuity equation:

$$\frac{\partial(S_a\rho_g E_g)}{\partial t} + \frac{\partial(S_a\rho_g E_g V_g)}{\partial z} = 0 \tag{6}$$

Liquid continuity equation:

$$\frac{\partial[S_a\rho_l(1-E_g)]}{\partial t} + \frac{\partial[S_a\rho_l(1-E_g)V_g]}{\partial z} = 0 \tag{7}$$

Gas-liquid two-phase hybrid equation:

$$\frac{\partial[S_a\rho_g E_g V_g + S_a\rho_l(1-E_g)V_l]}{\partial t} + \frac{\partial[S_a\rho_g E_g V_g^2 + S_a\rho_l(1-E_g)V_l^2]}{\partial z} + S_a\frac{\partial P}{\partial z} + S_a\left(\frac{\partial P}{\partial z}\right)_{fr} + S_a[\rho_g E_g + \rho_l(1-E_g)]g = 0 \tag{8}$$

where ρ_g and ρ_l (Kg/m^3) are the gas and liquid densities, re-

spectively; E_g is the air void; V_g and V_l (m/s) are the gas and liquid speeds, respectively; S_a (m^2) is the wellbore annulus cross-sectional area; and $\left(\frac{\partial P}{\partial z}\right)_{fr}$ (Pa/m) is the friction loss.

2. Numerical Calculation Methods of the Ttemperature Model and Gas-Liquid Flow and Kill Models

To calculate the differential equations, the gas-liquid flow and kill models were discretized as follows:

(1) Temperature model

Within the drill pipe:

$$\begin{aligned}&\frac{\pi[T_a(i,k)-T_p(i,k)]}{\frac{1}{h_{pi}(i,k)d_{pi}}+\frac{1}{h_{po}(i,k)d_{po}}+\frac{\ln(d_{po}/d_{pi})}{2\lambda_{dp}}}\\&-S_pV_p\rho_p(i,k)c_p(i,k)\frac{T_p(i,k)-T_p(i,k-1)}{\Delta z}\\&+Q_{cp}(i,k)=S_p\rho_p(i,k)c_p(i,k)\frac{T_p(i,k)-T_p(i-1,k)}{\Delta t}\end{aligned}\tag{9}$$

After finishing the formula:

$$A_1T_p(i,k)=B_1T_p(i-1,k)+C_1T_p(i,k-1)+D_1T_a(i,k)+F_1\tag{10}$$

where

$$A_1=\frac{\pi}{\frac{1}{h_{pi}(i,k)d_{pi}}+\frac{1}{h_{po}(i,k)d_{po}}+\frac{\ln(d_{po}/d_{pi})}{2\lambda_{dp}}}+\frac{S_pV_p\rho_p(i,k)c_p(i,k)}{\Delta z}+\frac{S_p\rho_p(i,k)c_p(i,k)}{\Delta t}\tag{11}$$

$$B_1=\frac{S_p\rho_p(i,k)c_p(i,k)}{\Delta t}\tag{12}$$

$$C_1=\frac{S_pV_p\rho_p(i,k)c_p(i,k)}{\Delta z}\tag{13}$$

$$D_1=\frac{\pi}{\frac{1}{h_{pi}(i,k)d_{pi}}+\frac{1}{h_{po}(i,k)d_{po}}+\frac{\ln(d_{po}/d_{pi})}{2\lambda_{dp}}}\tag{14}$$

$$F_1=Q_{cp}(i,k)\tag{15}$$

Wellbore annulus in the formation section:

$$\begin{aligned}&\frac{2\pi\lambda_f d_{co}U_a}{d_{co}U_af(t)+2\lambda_f}[T_f(i,k)-T_a(i,k)]\\&-\frac{\pi[T_a(i,k)-T_p(i,k)]}{\frac{1}{h_{pi}(i,k)d_{pi}}+\frac{1}{h_{po}(i,k)d_{po}}+\frac{\ln(d_{po}/d_{pi})}{2\lambda_{dp}}}\\&+S_aV_a\rho_a(i,k)c_a(i,k)\frac{T_a(i,k+1)-T_a(i,k)}{\Delta z}\\&+Q_{ca}(i,k)=S_a\rho_a(i,k)c_a(i,k)\frac{T_a(i,k)-T_a(i-1,k)}{\Delta t}\end{aligned}\tag{16}$$

After completion:

$$\begin{aligned}A_2T_a(i,k)=&B_2T_p(i,k)+C_2T_a(i-1,k)\\&+D_2T_a(i,k+1)+E_2T_f(i,k)+F_2\end{aligned}\tag{17}$$

where

$$\begin{aligned}A_2=&\frac{2\pi\lambda_f d_{co}U_a}{d_{co}U_af(t)+2\lambda_f}\\&+\frac{\pi}{\frac{1}{h_{pi}(i,k)d_{pi}}+\frac{1}{h_{po}(i,k)d_{po}}+\frac{\ln(d_{po}/d_{pi})}{2\lambda_{dp}}}\\&+\frac{S_aV_a\rho_a(i,k)c_a(i,k)}{\Delta z}\\&+\frac{S_a\rho_a(i,k)c_a(i,k)}{\Delta t}\end{aligned}\tag{18}$$

$$B_2=\frac{\pi}{\frac{1}{h_{pi}(i,k)d_{pi}}+\frac{1}{h_{po}(i,k)d_{po}}+\frac{\ln(d_{po}/d_{pi})}{2\lambda_{dp}}}\tag{19}$$

$$C_2=\frac{S_a\rho_a(i,k)c_a(i,k)}{\Delta t}\tag{20}$$

$$D_2=\frac{S_aV_a\rho_a(i,k)c_a(i,k)}{\Delta z}\tag{21}$$

$$E_2=\frac{2\pi\lambda_f d_{co}U_a}{d_{co}U_af(t)+2\lambda_f}\tag{22}$$

$$F_2=Q_{ca}(i,k)\tag{23}$$

Wellbore annulus in the water section:

$$\frac{\pi[T_s(i,k)-T_a(i,k)]}{\frac{1}{h_{ri}(i,k)d_{ri}}+\frac{1}{h_{io}(i,k)d_{io}}+\frac{\ln(d_{ro}/d_{ri})}{2\lambda_r}+\frac{\ln(d_{io}/d_{ii})}{2\lambda_i}}$$
$$-\frac{\pi[\mathrm{T_a}(i,k)-\mathrm{T_p}(i,k)]}{\frac{1}{\mathrm{h_{pi}}(i,k)\mathrm{d_{pi}}}+\frac{1}{h_{po}(i,k)d_{po}}+\frac{\ln(d_{po}/d_{pi})}{2\lambda_{dp}}}$$
$$+S_aV_a\rho_a(i,k)c_a(i,k)\frac{T_a(i,k+1)-T_a(i,k)}{\Delta z}$$
$$+Q_{ca}(i,k)=S_a\rho_a(i,k)c_a(i,k)\frac{T_a(i,k)-T_a(i-1,k)}{\Delta t} \quad (24)$$

After completion:

$$A_3T_a(i,k)=B_3T_p(i,k)+C_3T_a(i-1,k)+D_3T_a(i,k+1)+E_3T_s(i,k)+F_3 \quad (25)$$

where

$$A_3=\frac{\pi}{\frac{1}{h_{ri}(i,k)d_{ri}}+\frac{1}{h_{io}(i,k)d_{io}}+\frac{\ln(d_{ro}/d_{ri})}{2\lambda_r}+\frac{\ln(d_{io}/d_{ii})}{2\lambda_i}}+\frac{\pi}{\frac{1}{h_{pi}(i,k)d_{pi}}+\frac{1}{h_{po}(i,k)d_{po}}+\frac{\ln(d_{po}/d_{pi})}{2\lambda_{dp}}}+\frac{S_aV_a\rho_a(i,k)c_a(i,k)}{\Delta z}+\frac{S_a\rho_a(i,k)c_a(i,k)}{\Delta t} \quad (26)$$

$$B_3=\frac{\pi}{\frac{1}{h_{pi}(i,k)d_{pi}}+\frac{1}{h_{po}(i,k)d_{po}}+\frac{\ln(d_{po}/d_{pi})}{2\lambda_{dp}}} \quad (27)$$

$$C_3=\frac{S_a\rho_a(i,k)c_a(i,k)}{\Delta t} \quad (28)$$

$$D_3=\frac{S_aV_a\rho_a(i,k)c_a(i,k)}{\Delta z} \quad (29)$$

$$E_3=\frac{\pi}{\frac{1}{h_{ri}(i,k)d_{ri}}+\frac{1}{h_{io}(i,k)d_{io}}+\frac{\ln(d_{ro}/d_{ri})}{2\lambda_r}+\frac{\ln(d_{io}/d_{ii})}{2\lambda_i}} \quad (30)$$

$$F_3=Q_{ca}(i,k)\,. \quad (31)$$

(2) Gas-liquid flow and kill models

Gas continuity equation:

$$(S_aV_gE_g\rho_g)_{j+1}^{n+1}-(S_aV_gE_g\rho_g)_j^{n+1}=\frac{\Delta z}{2\Delta t}\left[\left(S_aE_g\rho_g\right)_j^n+\left(S_aE_g\rho_g\right)_{j+1}^n-\left(S_aE_g\rho_g\right)_j^{n+1}+\left(S_aE_g\rho_g\right)_{j+1}^{n+1}\right] \quad (32)$$

Liquid continuity equation:

$$(S_aV_lE_l\rho_l)_{j+1}^{n+1}-(S_aV_lE_l\rho_l)_j^{n+1}=\frac{\Delta z}{2\Delta t}\left[\left(S_aE_l\rho_l\right)_j^n+\left(S_aE_l\rho_l\right)_{j+1}^n-\left(S_aE_l\rho_l\right)_j^{n+1}+\left(S_aE_l\rho_l\right)_{j+1}^{n+1}\right] \quad (33)$$

Gas-liquid two-phase hybrid equation:

$$\begin{aligned}P_{j+1}^{n+1}-P_j^{n+1}=&\frac{\Delta z}{2\Delta t}[(\rho_gE_gV_g+\rho_lE_lV_l)_j^n+(\rho_gE_gV_g+\rho_lE_lV_l)_{j+1}^n\\&-(\rho_gE_gV_g+\rho_lE_lV_l)_j^{n+1}-(\rho_gE_gV_g+\rho_lE_lV_l)_{j+1}^{n+1}]\\&+[(\rho_gE_gV_g^{\,2}+\rho_lE_lV_l^{\,2})_j^{n+1}-(\rho_gE_gV_g^{\,2}+\rho_lE_lV_l^{\,2})_{j+1}^{n+1}]\\&-\frac{\Delta z}{2}\left\{[\rho_gE_gg+\rho_lE_lg]_j^{n+1}+[\rho_gE_gg+\rho_lE_lg]_{j+1}^{n+1}\right\}\\&-\frac{\Delta z}{2}\left\{\left[\left(\frac{\partial P}{\partial z}\right)_{fric}\right]_j^{n+1}+\left[\left(\frac{\partial P}{\partial z}\right)_{fric}\right]_{j+1}^{n+1}\right\}\end{aligned} \quad (34)$$

After completion:

$$P_{j+1}^{n+1}-P_j^{n+1}=M_A+M_B+M_C+M_D \quad (35)$$

where

$$\begin{aligned}M_A=\frac{\Delta z}{2\Delta t}[&(\rho_gE_gV_g+\rho_lE_lV_l)_j^n\\&+(\rho_gE_gV_g+\rho_lE_lV_l)_{j+1}^n\\&-(\rho_gE_gV_g+\rho_lE_lV_l)_j^{n+1}\\&-(\rho_gE_gV_g+\rho_lE_lV_l)_{j+1}^{n+1}]\end{aligned} \quad (36)$$

$$\begin{aligned}M_B=&(\rho_gE_gV_g^{\,2}+\rho_lE_lV_l^{\,2})_j^{n+1}\\&-(\rho_gE_gV_g^{\,2}+\rho_lE_lV_l^{\,2})_{j+1}^{n+1}\end{aligned} \quad (37)$$

$$\begin{aligned}M_C=&[\int(\rho_gE_gg+\rho_lE_lg)dz]_j^{n+1}]\\&-[\int(\rho_gE_gg+\rho_lE_lg)dz]_{j+1}^{n+1}]\\&-\frac{\Delta z}{2}\left\{[\rho_gE_gg+\rho_lE_lg]_j^{n+1}]+[\rho_gE_gg+\rho_lE_lg]_{j+1}^{n+1}]\right\}\end{aligned} \quad (38)$$

Table 1. Specifications of NH3-2.

Well depth/m	3630	Water depth/m	1298
Riser internal diameter/mm	482.6	Riser external diameter/mm	533.4
Delivery rat/(L/s)	27.1	Rotate speed/rpm	80
Initial viscosity/Pa.s	55	Bottom hole formation pressure/MPa	43.9
Drilling fluid density/(g/cm^3)	1.14	Geothermal gradient/(°C/m)	0.0463
Blowout preventer rated working pressure/MPa	103		

Table 2. Casing parameters.

Borehole size/mm	Casing external diameter/mm	Casing internal diameter/mm	Casing depth/m	Steel grade	Buckle type	Tensile strength/kN	Collapsing strength/MPa	Internal pressure strength/MPa
914.4	914.4	882.14	1407	X-56	D-90/MT D-60/MT	40495 /27391	18.55 /7.31	18.75 /28.13
660.4	508	482.6	2000	X-56	S-90/MT	9474	10.00	21.10
444.5	339.7	315.34	2800	N-80Q	SL-BOSS	6926	15.60	34.61
311.15	Open hole section		3625					

$$M_D = [\int (\frac{\partial P}{\partial z})_{fric} dz]_j^{n+1}] - [\int (\frac{\partial P}{\partial z})_{fric} dz]_{j+1}^{n+1}] - \frac{\Delta z}{2}\left\{\left[\left(\frac{\partial P}{\partial z}\right)_{fric}\right]_j^{n+1} + \left[\left(\frac{\partial P}{\partial z}\right)_{fric}\right]_{j+1}^{n+1}\right\}. \quad (39)$$

3. Calculation Method for Maximum Allowable Killing Casing Pressure

According to the offshore drilling manual (Dong et al., 2011), the maximum allowable killing casing pressure should not exceed the minimum value of the wellhead rated working pressure, 80% of the casing internal pressure strength, and permitted casing pressure by weak formation fracture pressure. Therefore, the maximum allowable killing casing pressure can be calculated as follows:

(1) Determine the wellhead rated working pressure, P_{wh}, according to the wellhead equipment type;
(2) Determine the casing internal pressure strength, P_{ci}, (i is the casing level) of various casing levels according to the cemented casing types. For two or more casing levels (not tieback liner), select the minimum value of each level's casing internal pressure strength;
(3) Determine the open hole formation fracture pressure, P_{fmin}, and its depth H according to the casing program and formation fracture pressure profile; and
(4) Determine the maximum allowable killing casing pressure, P_j, under various killing fluid density, ρ_j, according to the spare killing fluid density of various as follows:

$$P_j = \min\left\{P_{wh}, \min(0.8 \cdot P_{ci}), (P_{fmin} - \rho_j)\, 0.00981 \cdot H\right\}. \quad (40)$$

III. RESULTS AND DISCUSSION

In addition to equipment failure and human error, crucial factors such as formation pressure prediction error, timely warning of overflow value, and killing parameter (such as kill rate) design affect the gas cut and well killing safety. These factors can be quantified and evaluated through calculation and are conducive to dynamic risk assessment of gas cutting in deepwater drilling by analyzing the impact of these factors on well control risks.

To study the well control risks under various overflow rates, formation pressures, and kill rates, we calculated and analyzed the gas cutting and killing processes of deepwater well NH3-2 by using previously established methods (gas-liquid flow and well killing models in deepwater drilling and calculation method for maximum allowable killing casing pressure). The specifications of the deepwater well are presented in Table 1, and the open hole and casing parameters are presented in Table 2. Fig. 1 presents the casing program diagram.

Assuming that a gas cut occurs when drilling is performed till the bottom, the following can be obtained according to the methods described in Section 2.2:

$$P_{wh} = 103 \text{ MPa}; P_{c2} = 21.10 \text{ MPa};$$

the minimum fracture pressure exists at 2800 m, $P_{fmin} = 1.48$ g/cm^3.

Therefore, the maximum allowable killing casing pressure is given by

$$P_j = \min\{103, 0.8 \times 21.10, (1.48 - 1.14) \times 0.00981 \times 2800\} = \min\{103, 16.88, 9.34\} = 9.34 \text{ MPa}.$$

This indicates that CPC (casing pressure closed) should not exceed 9.34 MPa during killing in this deepwater well.

The models established in Section 2.1 can be used for si-

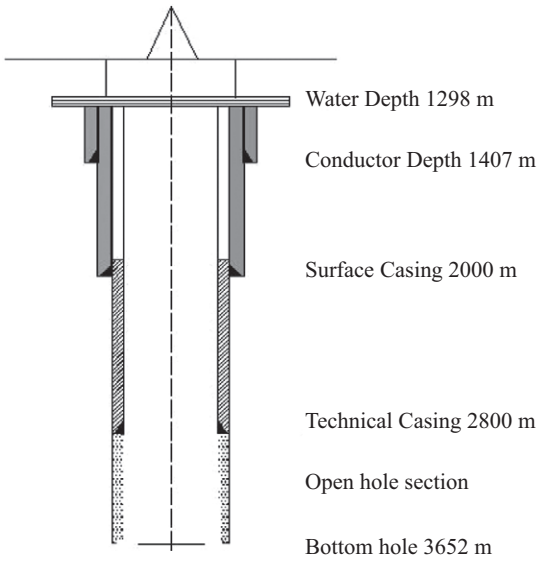

Fig. 1. Schematic of the casing program.

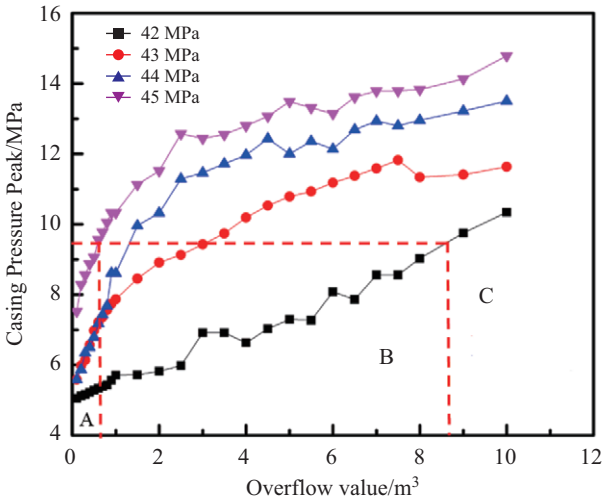

Fig. 2. Casing pressure peak changes with overflow rate under various formation pressures.

mulating the gas cutting and killing processes under various overflow rates, formation pressures, and kill rates and for analyzing the impact of various factors on well control risks.

1. Influence of Overflow Rate on Well Control under Various Conditions

The formation pressure prediction error increases under a deepwater environment. Assuming that the true value of formation pressure is between 42 and 45 MPa, the casing pressure peak changes with overflow rate were calculated under various formation pressures (42, 43, 44, and 45 MPa), as shown in Fig. 2.

The red horizontal line represents the maximum allowable killing casing pressure. As shown in the figure, Area A is safe against the formation prediction error, which indicates that the casing pressure peak will not exceed the maximum allowable

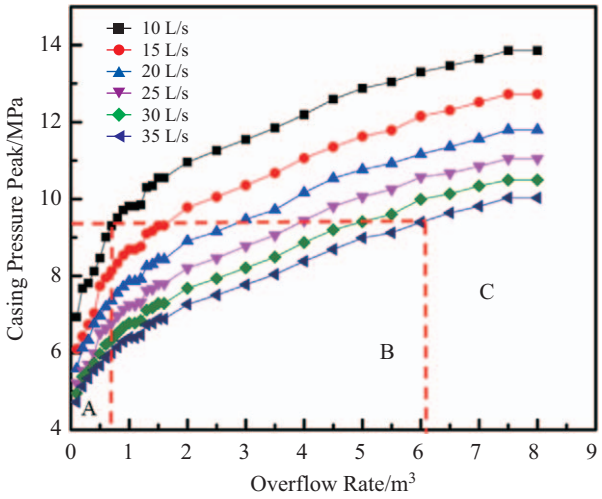

Fig. 3. Casing pressure peak changes with overflow rate under various kill rates.

killing casing pressure during well kill until the overflow rate exceeds 0.6 m^3. In Area B, various formation pressures correspond to various safe overflow rates. The higher the formation pressure, the lower the safe value of overflow rate, which indicates that a higher accuracy is required for the early detection of overflow in Area B. In Area C, the casing pressure peak exceeds the maximum allowable killing casing pressure under various formation pressures, which indicates that Area C is an absolutely dangerous region. In this area, the well control risk can markedly increase during a well kill if the overflow rate exceeds 8.4 m^3, which leads to killing failure.

When the gas cut is detected and the killing operation is performed, the kill rate is also essential for well control. The casing pressure peak changes with overflow rate under various kill rates (10, 15, 20, 25, 30, and 35 L/S) are presented in Fig. 3.

The three areas A, B, and C can still be observed in the figure. Area A with an overflow rate of < 0.6 m^3 is an absolutely safe region; Area B with an overflow rate of 0.6-6 m^3 is a conditional safe region. Various safe overflow values for various kill rates can be selected to determine the absolute safe region under the kill rate condition. Area C with an overflow rate of > 6 m^3 is an absolutely dangerous region. In this area, the well control risk can markedly increase during a well kill if the overflow rate exceeds 6 m^3, which leads to killing failure.

2. Influence of Formation Pressure on Well Control under Various Conditions

The casing pressure peak changes with formation pressure under various overflow rates (1, 2, 3, and 4 m^3) are presented in Fig. 4.

Similar to the description in Section 3.1, the maximum allowable formation pressure under a certain overflow rate condition can be determined from Fig. 4. The true value of formation pressure must be less than the maximum value; otherwise, it can increase the well control risk and can also lead to killing fails.

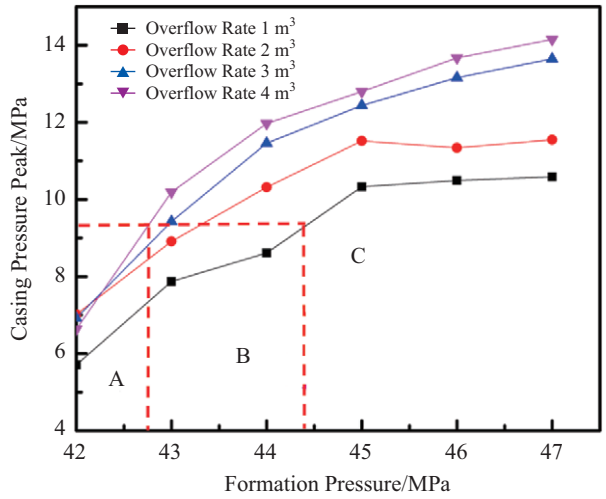

Fig. 4. Casing pressure peak changes with formation pressure under various overflow rates.

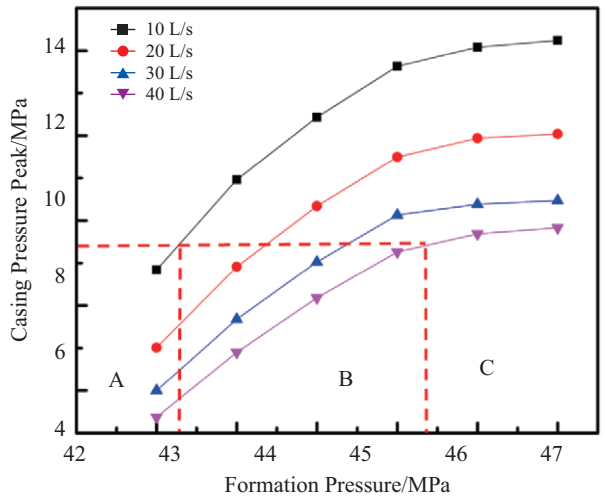

Fig. 5. Casing pressure peak changes with formation pressure under various kill rates.

Thus, the accuracy of the overflow monitoring equipment and formation pressure prediction can be combined to assess the gas cutting risk in well control.

The casing pressure peak changes with formation pressure under various kill rates (10, 20, 30, and 40 L/S) are presented in Fig. 5.

From Fig. 5, the maximum allowable formation pressure under a certain kill rate condition can be determined. The true value of formation pressure must be less than the maximum value; otherwise, it can increase the well control risk and can also lead to killing fails. Thus, the accuracy of formation pressure prediction and alternative kill rate solutions can be combined to assess the gas cutting risk in well control.

3. Influence of Kill Rate on Well Control under Various Conditions

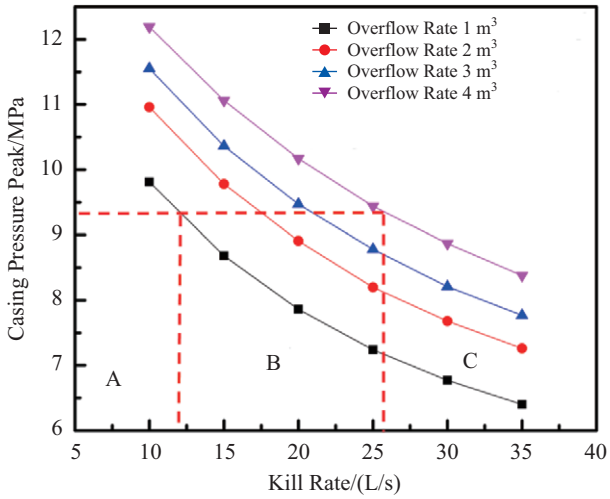

Fig. 6. Casing pressure peak changes with kill rate under various overflow rates.

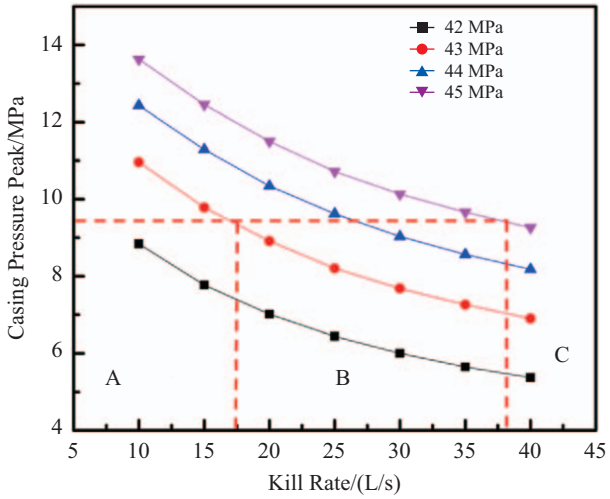

Fig. 7. Casing pressure peak changes with kill rate under various formation pressures.

The casing pressure peak changes with kill rates under various overflow rates (1, 2, 3, and 4 m^3) are presented in Fig. 6.

From Fig. 6, the minimum allowable kill rate under a certain overflow rate condition can be determined. The kill rate used must be more than the minimum value; otherwise, it can cause the casing pressure peak to exceed the maximum allowable killing casing pressure and increase the well control risk, which can also lead to killing fails. Thus, the accuracy of overflow monitoring equipment can be combined to recommend a rational killing rate and reduce the well control risk.

The casing pressure peak changes with kill rate under various formation pressures (42, 43, 44, and 45 MPa) are presented in Fig. 7.

From Fig. 7, the minimum allowable kill rate under a certain formation pressure condition can be determined. The kill rate used must be more than the minimum value; otherwise, it can

cause the casing pressure peak to exceed the maximum allowable killing casing pressure and increase the well control risk, which can also lead to killing fails. Thus, the accuracy of formation pressure prediction can be combined to recommend a rational killing rate and reduce well control risks.

IV. CONCLUSION

(1) By calculating the maximum allowable killing casing pressure, the well control risks under various overflow rates, formation pressures, and kill rates were analyzed, and a well control capacity-based risk analysis method for gas cutting in deepwater drilling was established.
(2) The method established in this paper considers the well control capacity under various drilling conditions and analyzes the well control risk after a gas cut against various conditions to recommend the safe construction parameter range and overflow monitoring index.
(3) Through calculation and example analysis, the timely warning of overflow rate, formation pressure prediction error, and kill rate were found to have a strong influence on the casing pressure peak in the killing process. The well control risks can be dynamically evaluated when combined under actual conditions, and parameters such as timely warning of overflow rate and kill rate can be optimized.

ACKNOWLEDGEMENTS

The authors would like to acknowledge the academic and technical supports of China University of Petroleum (East China) and China University of Petroleum (Beijing). This paper is supported by the National Natural Science Foundation of China (No. 51574275) and the National Science Fund for Distinguished Young Scholars (No. 51325402), and also supported by Ministry of education innovation team development plan rolling support project (IRT_14R58).

REFERENCES

Avelar, C. S., P. R. Ribeiro and K. Sepehrnoori (2009). Deepwater gas kick simulation. Journal of Petroleum Science & Engineering 67, 13-22.

Botrel T. and P. Isambourg (2001). Off setting kill and choke lines friction losses, a new method for deep water well control. Offshore Drilling, SPE-67813.

Chen, P. and T. Ma (2014). Research staus of early monitoring technology for deepwater drilling overflow. Petroleum Research 3, 602-612.

Chu, D. (2012). Well control technology in deepwater well. Petroleum Drilling Techniques.

David, H., J. Stuart and J. Ben (2001). Early kick detection for deepwater drilling: New probabilistic methods applied in the field. Spe Annual Technical Conference & Exhibition, SPE-71369.

Dong, X., S. Cao and H. Tang (2011). Offshore Drilling Manual. Petroleum Industry Press.

Gao, Y., B. Sun, Z. Wang, S.-J. Cao, L.-S. Song and H.-Q. Cheng (2008). Calculation and analysis of wellbore temperature field in deepwater drilling. Journal of China University of Petroleum: Edition of Natural Science 32(2), 58-62.

Gupta, V., J. D. Dhameliya and S. Jain (2013). Liquid lift dual gradient drilling in deep water: early kick detection and control. Spe Western Regional & Aapg Pacific, SPE-165372.

Johnson, A., C. Leuchtenberg, S. Petrie and D. Cunningham (2014). Advancing deepwater kick detection. Society of Petroleum Engineers, SPE-167990.

Kerr, R. A. (2010). Gulf oil disaster. How to kill a well so that it's really most sincerely dead. Science 329(5987), 23.

Khain, V. E. and I. D. Polyakova (2004). Oil and gas potential of deep- and ultradeep-water zones of continental margins. Lithology & Mineral Resources 39(6), 530-540.

Luo, Y., M. Chen, Y. Jin, M. Du and J. Hou (2011). Well kill technique for abnormal high formation pressure in Well Arvand-1 of Iran. Petroleum Drilling Techniques.

Meng, Y., C. Xu, N. Wei, G. Li, H. Li and M. Duan (2015). Numerical simulation and experiment of the annular pressure variation caused by gas kick/injection in wells. Journal of Natural Gas Science & Engineering 22, 646-655.

Ning, L. (2008). The Effects of Drilling Fluid's Physical Properties on the Temperature and Pressure in Deepwater Drilling. China University of Petroleum.

Ren, M. P. , X. F. Li, D. R. Xu and B. T. Yin (2012). Research of kick and distribution features of gas-liquid two phase flow during drilling. Journal of Engineering Thermophysics 33(12), 2120-2125.

Ren, M. P. and X. F. Li (2011). The characteristics and identification method of gas-liquid two flow overflow in deepwater drilling. Journal of Engineering Thermophysics 32(12), 2068-2072.

Song, X. (2011). Full transient analysis of heat transfer during drilling fluid circulation in deep-water wells. Acta Petrolei Sinica 32(4), 704-708.

Sun, L., Z. Guan, H. Liang and M. Jiang (2013). Effects of casing program change and liner tieback on well control. Petroleum Drilling Techniques 41(6), 34-39.

Xu, Y., Z. Guan and K. Su (2014). Methods of setting depth range with credibility of conductor for deepwater drilling based on probability statistics. Applied Ocean Research 48, 301-307.

Xu, Y., Z. Guan, H. Zhang, H. Zhang and K. Wei (2014). Analysis of the impact of managed pressure drilling technology on current casing program design methods. International Journal of Engineering 27(4) ,1025-2495.

Zhou, B., J. Yang, B. Zhang, H. Tang, J. Luo and Y. Wang (2012). Prediction and control technology of shallow geological hazards in deepwater area. Marine Geology Frontiers.

Zhou, Q., H. Zhao, H. Zhan, H. Zhang and C. H. Lu (2013). The application of ultrasonic based on Doppler effect used in early kick detection for deep water drilling. Communications, Circuits and Systems (ICCCAS), 2013 IEEE International Conference 2, 488-491.

Zhuo, L., Y. Ge and H. Wang (2009). Early kick detection methods for deepwater drilling and its future development. Oil Drilling & Production Technology.